frontiers | Frontiers in Materials

TYPE Original Research
PUBLISHED 20 October 2025
DOI 10.3389/fmats.2025.1676801

OPEN ACCESS

EDITED BY
Changtai Zhou,
City University of Hong Kong, Hong Kong, SAR China

REVIEWED BY
Mao Xuwei,
Inner Mongolia University of Science and Technology, China
Xizhi Wang,
Hunan University of Science and Technology, China
Lv Jiakun,
Jiangsu University of Science and Technology, China
Jie Ren,
Inner Mongolia University of Technology, China

*CORRESPONDENCE
Yanbin Yang,
2712182683@qq.com

RECEIVED 31 July 2025
ACCEPTED 16 September 2025
PUBLISHED 20 October 2025

CITATION
Yang Y, Gu W, Fang J, Zhang S and Zhang B (2025) Evaluation of rock burst hazard in fully mechanized mining face and separate source prevention and control technology. *Front. Mater.* 12:1676801. doi: 10.3389/fmats.2025.1676801

Evaluation of rock burst hazard in fully mechanized mining face and separate source prevention and control technology

Yanbin Yang[1]*, Wenzhe Gu[1], Jialiang Fang[2], Shuai Zhang[3] and Beiyan Zhang[1]

[1]China Coal Energy Research Institute Co., Ltd., Xi'an, China, [2]China Railway 17th Bureau Group Second Engineering Co., Ltd., Xi'an, China, [3]College of Energy and Mining Engineering, Xi'an University of Science and Technology, Xi'an, China

To ensure safe and efficient mining at the 41,109 working face of Dafosi Mine, a systematic study was conducted focusing on key issues in rockburst prevention and control, using the 41,109 working face as the research context. First, an analysis of rockburst influencing factors was performed, proposing the use of a comprehensive index method to evaluate the rockburst hazard level of the working face. Based on the evaluation results, the working face was further divided into rockburst hazard zones. A source-specific monitoring and early warning system for rockburst was established targeting different hazard sources, accompanied by corresponding prevention and control measures. The research results show that when the comprehensive index method is applied to evaluate the rock burst risk of the 41,109 working face in Dafosi Coal Mine by considering both geological and mining factors, the risk evaluation index is 0.429, corresponding to a weak rock burst risk level. Centering on the two primary shock-inducing factors—roof dynamic loading and surrounding rock static loading—a source-specific monitoring and early warning system combining "regional monitoring + localized monitoring" was successfully established. By rationally deploying microseismic monitoring equipment, acoustic emission devices, and borehole stress monitoring systems, a source-specific prevention plan for the working face was designed. Ultimately, deep-hole pre-blast and large-diameter borehole pressure-relief measures were implemented on the roof. Concurrently, microseismic equipment monitored effectiveness, reducing microseismic energy by 54% compared to pre-treatment levels. This effectively controlled rockburst risks, ensuring safe and efficient mining operations at the working face with excellent on-site application results.

KEYWORDS

rock burst, comprehensive index method, separate source prevention and control, microseismic monitoring, pre-splitting blasting

1 Introduction

As the primary energy source in my country's energy security system, coal occupies an irreplaceable strategic position in ensuring national economic development and energy structure stability (Qi et al., 2019). However, the complex geological conditions of deep coal seams, influenced by factors such as increased ground stress, frequent tectonic activity,

and changes in the physical and mechanical properties of coal and rock masses, have led to a high frequency and prevalence of dynamic hazards such as rock bursts (Zhang et al., 2025a; Zhang et al., 2025). Rock bursts, a typical coal mine dynamic hazard, are essentially the sudden instability and failure of coal and rock masses under high stress, instantly releasing large amounts of elastic potential energy. This not only poses a serious threat to coal mine safety and production, but also reduces mining efficiency and causes huge economic losses. It has become a core bottleneck restricting the safe and efficient mining of deep coal resources (Pan et al., 2021; Zhang et al., 2026; Ming, 2024). Therefore, exploring rock burst monitoring, early warning, and prevention technologies suitable for thick and hard roof conditions has important theoretical significance and engineering value.

To address the challenges of rock burst prevention and control, domestic and international scholars have conducted extensive and systematic research on its occurrence mechanisms, monitoring and early warning, and pressure relief and disaster relief technologies, achieving fruitful results (Cao et al., 2025; Zhang et al., 2024a; Tan et al., 2024). In terms of mechanism and early warning research, Linming et al. (2021), Linming et al. (2017) and Linming et al. (2015) based on the "stress-energy" coupling theory, integrated multi-source data such as mine microseismic, ground sound, and stress monitoring to construct a multi-parameter collaborative early warning indicator system. Through big data analysis, they achieved dynamic classification of rock burst hazards, effectively improving the timeliness of disaster warnings. He et al. (2020) analyzed the prying effect of rock pillars on site and combined it with the collection of microseismic data on site to analyze the causes of rock burst in steeply inclined coal seams and proposed relevant targeted measures. Wang et al. (2017) studied the main causes, mechanisms, and characteristics of rock burst in the Yima mining area from multiple perspectives and factors in the complex geological environment of the Yima coalfield, providing a basis for further detailed analysis of the rock burst formation mechanism. Lu et al. (2019) studied the various anisotropic characteristics of coal body rock burst tendency from the perspective of structural weak planes such as bedding, providing theoretical support for in-depth analysis of the rock burst mechanism from a microscopic perspective. Qiu et al. (2025) used the BPM-DFN coupling method to explore the dynamic tensile behavior of jointed rock masses under different loading rates and joint densities. Their results provide theoretical support for understanding the mechanisms of rock burst, assessing hazardous areas, and optimizing pressure relief and prevention technologies. Yongxue et al. (2011) proposed a combined microseismic and geoacoustic monitoring technology for the thick, hard roof conditions of a deep mine. Leveraging the complementary nature of the two technologies at different monitoring scales (microseismic monitoring of large-energy events in the region, while geoacoustic detection of small, local disturbances), they achieved preliminary multidimensional identification of impact precursors. Yuan (2020) leveraging big data and data mining techniques, established a model for identifying coal mine dynamic disaster risks, quantifying factors such as mining geological conditions and production disturbances, providing theoretical support for the proactive prediction of impact hazards. Zhou et al. (2025) employed a particle flow model to study the mechanical response of fractured rock masses under dynamic tensile loading, revealing the mechanisms by which fracture density, inclination, and distribution influence fracture patterns and energy release patterns.

In the field of pressure relief technology, Lai et al. (2025) systematically compared the energy evolution patterns of high-energy-storage rock under modification and control using a "full-process" versus a "staged" approach, revealing the dynamic impact of modification measures on rock energy storage and release behavior. Feng et al. (2019) revealed the energy release law of hard roof rupture through similar simulation tests and field measurements, clarified the mechanical mechanism of roof rupture-induced rock burst, and optimized the parameters of deep-hole blasting of the roof accordingly; in addition, technologies such as large-diameter drilling and hydraulic fracturing to relieve pressure in coal bodies have also been widely used on site and have become the main means to alleviate the high stress state of coal and rock masses. Liu et al. (2017) achieved active regional prevention and control to a certain extent by implementing the technology of first fracturing (secondary destruction) and then grouting (soft rock hardening). Xie et al. (2017) proposed a revolutionary concept to implement "fluidized mining" technology for deep coal in the future, which subverted the original traditional mining method. According to the concept, the problem of rock burst can be solved to a certain extent in the future.

Although existing research has achieved some success in the "empirical judgment - real-time monitoring - pressure relief and crisis resolution" technical system, certain limitations still exist in practical application. On the one hand, while combined microseismic and geoacoustic monitoring can achieve regional and local complementarity, it is limited by frequency band overlap, positioning errors, and missed events, and has not yet formed an operational standard for identifying dynamic and static load sources (Kong et al., 2024; Dai et al., 2025). On the other hand, pressure relief measures such as deep hole blasting or large-diameter drilling rely heavily on experience in parameter design and lack quantitative basis. Furthermore, insufficient dynamic feedback after implementation makes it difficult to optimize measures (Huicong et al., 2022; Zhang et al., 2005b). Therefore, exploring rock burst monitoring, early warning, and prevention technologies suitable for deep, thick, and hard roof conditions has important theoretical significance and engineering value (Zhang et al., 2024b; Yang et al., 2024; Pengxiang et al., 2024; Pan et al., 2024).

Based on this, this paper uses the 41,109 mining face of a certain mine as an engineering context to systematically analyze the main factors influencing rock burst. Using a comprehensive index method, it assesses rock burst risk and delineates risk zones. Based on this, a source-based monitoring system (regional microseismicity, localized ground sound, and borehole stress) is constructed. Targeted prevention and control measures are proposed, and their effectiveness is verified through field testing.

2 Analysis of engineering context and factors influencing rock burst

2.1 Mine mining conditions

Dafosi Coal Mine is located in the south of Binchang Mining Area, Shaanxi Province, with a length of 14 km from east to west, a width of 6.5 km from north to south, and an area of 71.2931 km^2.

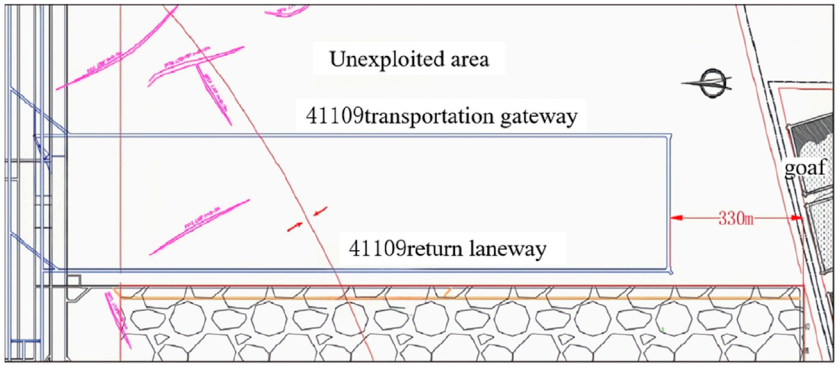

FIGURE 1
Engineering background and analysis of influencing factors of rock burst.

There are two minable coal seams in the mine field, namely, No. 4 coal seam and No. 4 upper coal seam. The main mining seam is No. 4 coal seam, with an average thickness of 11.65 m, which is an extra-thick coal seam with stable and relatively hard properties. The No. 4 upper coal seam is the upper split seam of No. 4 coal seam, which is locally minable with an average thickness of 2.88 m. The strike longwall fully mechanized mining method was adopted, and the roof was managed by the natural caving method.

The 41,109 working face mainly mined the No. 4 upper coal seam, which is a medium-thick coal seam with 1–2 layers of gangue locally. The strike length of the working face was 1,481 m, the dip length was 290 m, and the area was 429,490 m^2. The north of the working face was the west development roadway, the south was 300 m away from the goaf of No. 4 coal seam in Jiangjiahe Mine Field, the east was solid coal, the west of No. 4 upper coal seam was solid coal, and the No. 4 coal seam was the goaf of 40,202 working face. The No. 4 upper coal seam was 36 m above the No. 4 coal seam. The plane layout of the 41,109 working face was shown in Figure 1.

2.2 Analysis of main influencing factors of rock burst in working face

2.2.1 Rock burst tendency of coal and rock strata

To identify whether rock burst disasters will occur in the working face, the first thing to consider is whether the surrounding rock near the working face has rock burst tendency. As one of the necessary conditions for the occurrence of rock burst, the identification results should be comprehensively considered with factors such as coal seam occurrence, mining technology, mining conditions, and support characteristics near the working face. Because there are many forms of rock burst disasters, specific analysis is required to put forward targeted control technologies. If the identification result is medium or above, standardized operations, reasonable layout, risk consideration, and safety measures formulation should be carried out during mining. This is because there are many occurrence conditions, which are closely related to geological and mining factors. According to the rock burst tendency identification results (see Table 1), the coal seam and roof of the 41,109 working face during mining had weak rock burst tendency, while the floor did not have rock burst tendency. During mining, attention should be paid to the impact of the roof and coal seam on safe mining.

TABLE 1 Identification results of coal and rock mass impact tendency in 41,109 working face.

Lithology	Identification index				Identification result
	DT	W_{ET}	K_E	R_C	
4^{upper}Coal	237.8	20.487	1.705	13.383	Type II
Roof	U_{WQ} = 105.128 kJ				Type II
Floor	U_{WQ} = 10.860 kJ				Type I

2.2.2 Mining depth

Regarding the definition of coal seam mining depth, the traditional view holds that when the mining depth exceeds 500 m, the coal seam is considered to enter deep mining. However, Xie et al. (2012) proposed to define the mining depth from the perspective of stress environment. With the increase of depth, the risk coefficient of rock burst disasters changes nonlinearly. Studies have shown that the stress environment of surrounding rock changes significantly with the increase of mining depth. Even in different mining areas of a mine field, the possibility of rock burst varies greatly. According to the distribution of coal seam burial depth in the working face area, the coal seam depth in the mining range of the 41,109 working face of Dafosi Coal Mine was 436–521 m. According to the engineering analogy of mines with known rock burst occurrences, the burial depth of the 41,109 working face had reached the critical depth for rock burst occurrence, and the risk of rock burst was greatly increased.

2.2.3 Fault structure

Faults are one of the potential influencing factors of rock burst. Their existence destroys the overall continuity of rock strata, increases local stress distortion, and the stress state of faults is prone to sudden changes under the influence of mining disturbance,

10.3389/fmats.2025.1676801

TABLE 2 Classification table for dangerous state of rockburst.

Rock burst hazard level	Rock burst hazard state	Comprehensive index of rock burst hazard
A	Nothing	$W_t \leq 0.25$
B	weak	$0.25 < W_t < 0.5$
C	Medium	$0.5 < W_t < 0.75$
D	Strong	$W_t > 0.75$

TABLE 3 Geological factors and rock burst hazard index during mining period of 41,109 working face.

Factor	Rock burst influencing factors and evaluation indexes		Rock burst hazard index of 41,109 working face
	Factor description	Maximum index value	
W_1	Number of rock burst occurrences in the same coal seam	3	0
W_2	Mining depth/m	3	1
W_3	Distance from hard and thick roof strata to coal seam	3	0
W_4	Tectonic stress concentration coefficient in mining area/%	3	2
W_5	Thickness characteristic parameter of roof strata	3	2
W_6	Uniaxial compressive strength of coal seam/MPa	3	1
W_7	Elastic energy index of coal seam	3	3
$W_{t1} = \sum W_i / \sum W_{i\max}$			0.429

TABLE 4 Risk index of rock burst caused by mining factors during the mining period of 41,109 working face.

Factor	Rock burst influencing factors and evaluation indexes		Rock burst hazard index of 41,109 working face
	Factor description	Maximum index value	
W1	Relationship with adjacent goafs	3	1
W2	Length of working face/m	3	1
W3	Width of section coal pillar/m	3	3
W4	Thickness of residual bottom coal/m		
W5	Distance between final mining line and goaf	3	0
W6	Distance coefficient between working face and fault (with drop greater than 3 m)/%	3	1
W7	Distance between working face and structure/m	3	0
W8	Distance Lb between working face or roadway advancing towards the part where coal seam is eroded, merged, or with thickness change and the part where coal seam changes	3	0
$W_{t1} = \sum W_i / \sum W_{i\max}$			0.250

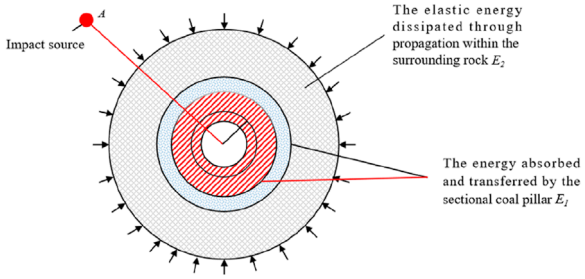

FIGURE 2
Energy dissipation model of coal pillars under dynamic-static load superposition effects.

resulting in unclear law of mining-induced stress in mining working faces, which is very easy to cause rock burst hazard. Field investigation found that there were two main faults, DF14 and FX13, in the east of the working face, among which the closest distance between the FX13 fault and the return airway was 30 m.

2.2.4 Width of section coal pillar

Due to the influence of the mining sequence of adjacent working faces, stress concentration is easily formed in section coal pillars. The stress superposition of adjacent working faces increases the stress concentration degree of coal mass near the coal pillar, so rock burst is most likely to occur near the coal pillar. A 30 m coal pillar was left between the return airway of the No. 4 upper coal seam 41,109 working face and the goaf of the No. 4 coal seam 40,202 working face, and the distance between the No. 4 upper coal seam and the No. 4 coal seam in this area was 36 m. According to the actual excavation situation of the 41,109 return airway (adjacent to the goaf), the integrity of the roadway surrounding rock was less affected by the roof caving of the 40,202 goaf, but the lateral abutment pressure of the 40,202 goaf had a certain impact on the 41,109 working face during mining, and local stress concentration was easy to occur in the coal pillar, which increased the rock burst hazard.

3 Evaluation of rock burst hazard level in working face

3.1 Rock burst hazard assessment method

The comprehensive index method has the characteristics of considering various factors, simple operation, and clear distinction. At present, the comprehensive index method is preferred to evaluate the rock burst hazard of the working face. The factors causing disasters can be divided into two categories: geological factors and mining factors. Each category can be divided in detail, and each sub-category has different contribution rates to the occurrence of disasters. To distinguish and evaluate the impact degree of various factors on rock burst disasters, a rock burst hazard evaluation and prediction system was established by using the weight analysis of the comprehensive index method. It could correctly understand the impact degree of rock burst on safe mining, which was convenient for the optimization of subsequent prevention and control measures.

$$W_t = \max\{W_{t1}, W_{t2}\} \tag{1}$$

Where, W_t—comprehensive index for evaluating the rock burst hazard level of the working face; W_{t1} —evaluation index of geological factors for the rock burst hazard level; W_{t2} —evaluation index of mining factors for the rock burst hazard level.

To refine the impact degree of geological factors and mining factors on the occurrence of rock burst, Formulas 2, 3 were introduced to calculate them respectively, and the final calculation results were taken as the judgment index for predicting the rock burst occurrence level.

$$W_{t1} = \sum_{i=1}^{n_1} W_i / \sum_{i=1}^{n_1} W_{i\max} \tag{2}$$

$$W_{t2} = \sum_{i=1}^{n_2} W_i / \sum_{i=1}^{n_2} W_{i\max} \tag{3}$$

3.2 Evaluation of rock burst hazard level in working face

A rock burst hazard evaluation method for the 41,109 working face was established based on the comprehensive index method, and the rock burst hazard evaluation levels were determined, as shown in Table 2. The rock burst hazard could be divided into four levels: no, weak, medium, and strong. Corresponding prevention and control measures were taken according to different rock burst hazard levels.

According to the rock burst hazard state classification table, combined with field investigation data and the rock burst tendency identification results of the coal seam, the contribution rate of geological factors to rock burst disasters was evaluated, and the final evaluation results were shown in Table 3.

According to the mining conditions, the relationship with adjacent goafs, the width of section coal pillars, and the distance characteristics of geological structures, the contribution value and evaluation results of mining factors to rock burst disasters were determined, as shown in Table 4.

Based on the above analysis and the aforementioned evaluation results, the comprehensive geological factors and mining technical factors were considered for the rock burst hazard during the mining period of the 41,109 working face. According to Formula (1), the highest hazard level was selected as the final rock burst hazard evaluation index, which was 0.429. The evaluation result of the rock burst hazard during the mining period of the 41,109 working face was weak.

3.3 Stress evolution characteristics under combined dynamic and static loading

Based on the previous study of the rock burst hazard index during the mining period of the 41,109 working face, it was found that the sectional pillar width poses a relatively high risk of rock burst in the working face. Guided by the principle of dynamic and

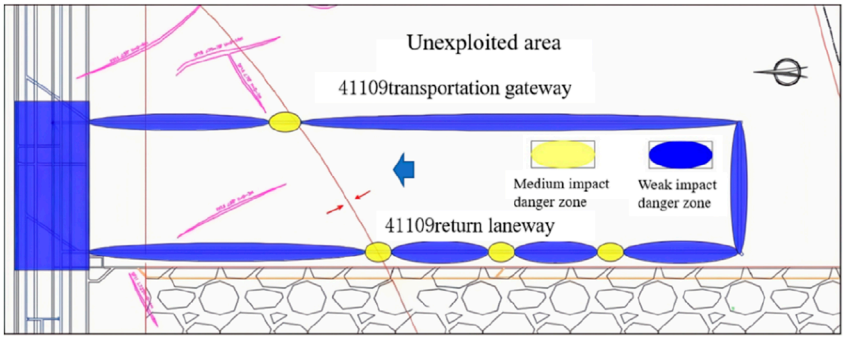

FIGURE 3
Classification of impact hazardous areas in 41,109 working face.

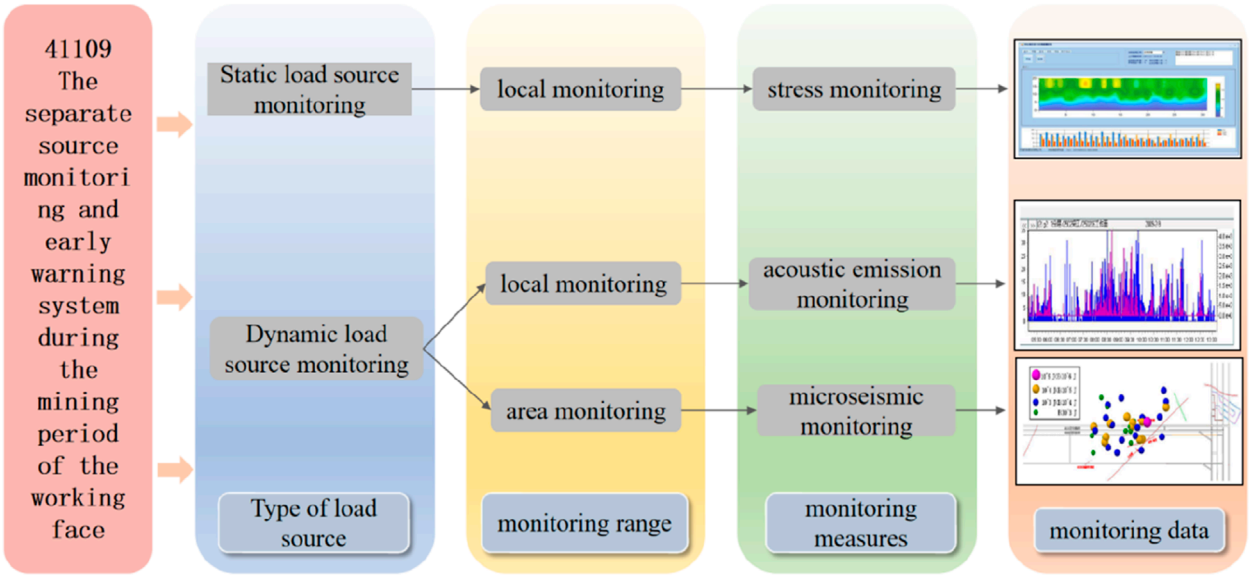

FIGURE 4
Monitoring and early warning system for ground impact sources in 41,109 working face.

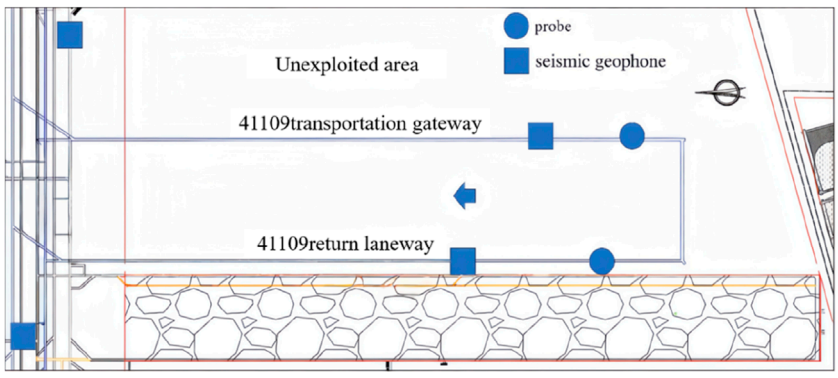

FIGURE 5
Layout of microseismic monitoring system for working face.

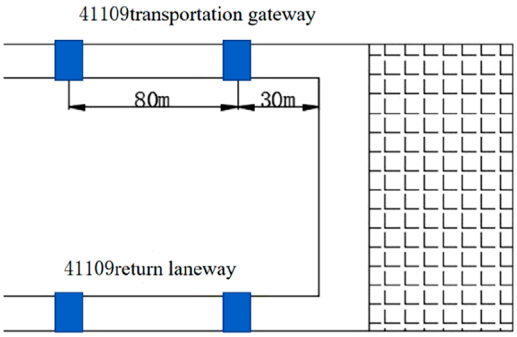

FIGURE 6
Layout of the ground sound monitoring system for the working face.

static load energy superposition, this study investigates the load-bearing stability of pillars in the working face section from a systemic energy perspective. The objective is to identify the critical conditions for tunnel impact instability, laying the foundation for subsequent development of rock burst prevention and control technologies for working faces.

Analyzing the distribution and transfer patterns of energy within the surrounding rock system is fundamental to identifying critical conditions for tunnel impact instability. Treating the tunnel as an independent entity, stress concentration and transfer occur under the influence of mining disturbances and energy release from roof fractures. Concurrently, internal energy changes occur alongside stress transfer, with energy concentration and release determining the stability of surrounding rock structures on both sides of the tunnel and the severity of impact hazards. The occurrence of rockburst can be simplified as follows: when the accumulated energy around the tunnel exceeds the energy dissipated by the sectional coal pillar and the accumulated energy on the solid coal side, the remaining undissipated and untransferred energy is released as impact kinetic energy (the energy causing tunnel instability and failure). Assuming the elastic energy accumulated in the roadway's composite load-bearing system is E_0, the energy absorbed and transferred by the sectional coal pillar is E_1, the elastic energy dissipated through propagation within the surrounding rock is E_2, the residual kinetic energy released is E_3, and the critical value for roadway instability and failure is E_{mix}, then:

$$E_3 = E_0 - E_1 - E_2 = \frac{1}{2}mv^2 \le E_{\lim} \tag{4}$$

In the formula: m represents the mass of the rock mass destroyed under impact loading, kg; v denotes the velocity of the rock mass destroyed under impact loading at the critical layer, m/s.

As shown in Equation 4, to prevent tunnel instability and failure after impact loading, the energy absorption and transfer characteristics of the sectional coal pillar can be utilized. Reducing the width of its plastic zone enhances its inherent stability, thereby strengthening its energy absorption and transfer capacity and eliminating the destructive effects of residual energy on the tunnel. The specific characteristics of internal energy transfer, absorption, and release within the composite support system for tunnel surrounding rock are illustrated in Figure 2.

Subjected to mining disturbances, the coal pillar remains under high static load. Following the release of impact loads from fractures in the critical overburden layer, the pillar assumes the primary load-bearing and resistance function. The exposed surfaces on both sides of the pillar undergo deformation due to the inclination support pressure from the mining face.

Assuming the deformation of the coal pillar adjacent to the goaf is $\Delta S(t)$ (where deformation is a function of impact duration t), and the deformation of the coal pillar adjacent to the roadway is $\Delta S'(t)$, then the internal deformation of the coal pillar is $\Delta S(t) + \Delta S'(t)$. The tensile resistance provided by the internal structure of the coal pillar is $F_{(t)}$, where the magnitude of $F_{(t)}$ primarily depends on the width and strength of the coal pillar. The energy absorbed and transferred by the sectional coal pillar, which bears the primary load-bearing capacity, consists of two main components: first, the energy E_{C1} absorbed by the pillar itself; second, the energy E_{C2} dissipated through the expansion of the plastic zone during the load-bearing process. According to Formula 5, the total energy E_1 absorbed and transferred by the pillar is given by the following relationship:

$$E_1 = E_{C1} + E_{C2} \tag{5}$$

$$E_{C1} = \int_0^t F(t)dt \tag{6}$$

$$E_{C2} = \int_0^t dt \int_0^{\Delta r(t)+\Delta R(t)} F(t)dr \tag{7}$$

If the coal pillar itself possesses high strength and good toughness, it will effectively absorb energy transferred from the overburden during load-bearing, maintaining a high overall support capacity $F_{(t)}$. When critical layers of the overburden fracture during mining, the released energy propagates downward as stress waves reaching the coal pillar, subjecting it to intense dynamic loading. This accelerates the expansion of the pillar's plastic zone, diminishing its energy absorption and transfer capacity. Therefore, to enhance the overall support capacity of the coal pillar and strengthen its energy absorption and transfer capabilities, it is essential to control the expansion rate and depth of the plastic zone. The support capacity of the coal pillar weakens as the mining process affects the development of discontinuities such as joints and fractures within the plastic zone, reducing the absorption and transfer of dynamic load energy. When intense disturbances from overburden fractures propagate to the coal pillar, the entire load-bearing structure shifts toward free space, according to Formula 6, causing E_{C1} to decrease. At this point, the expansion rate of the coal pillar's plastic zone accelerates, according to Formula 7, E_{C2} gradually diminishes, and the coal pillar's load-bearing capacity consequently declines.

In summary, during normal mining operations at the longwall face, the coal pillar undergoes compression deformation and edge fissure development under the influence of inclined support pressure, resulting in significant stress concentration. When concentrated stress exceeds the coal pillar's ultimate strength, stress peaks migrate deeper into the elastic zone while the plastic zone expands downward. This progressively reduces the width of the elastic bearing zone, increasing the likelihood of overall instability in the coal pillar's load-bearing region. When the

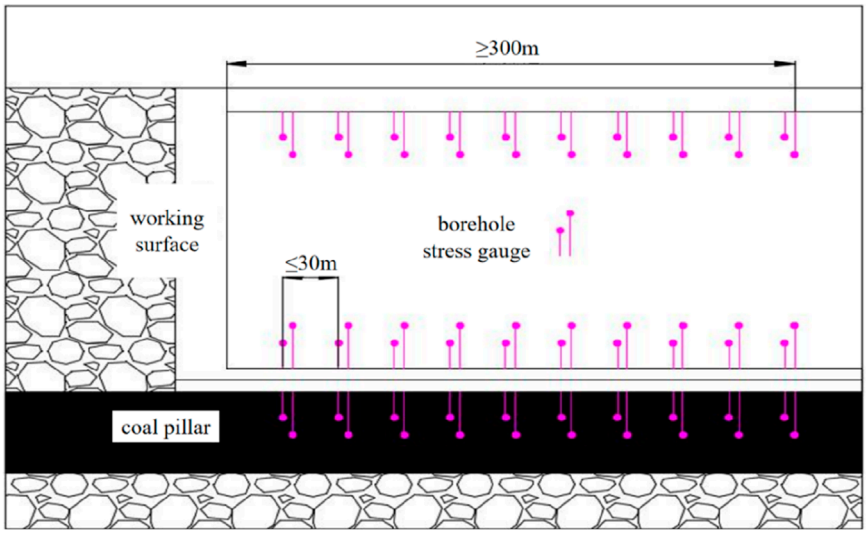

FIGURE 7
Layout of stress monitoring for drilling holes in the working face.

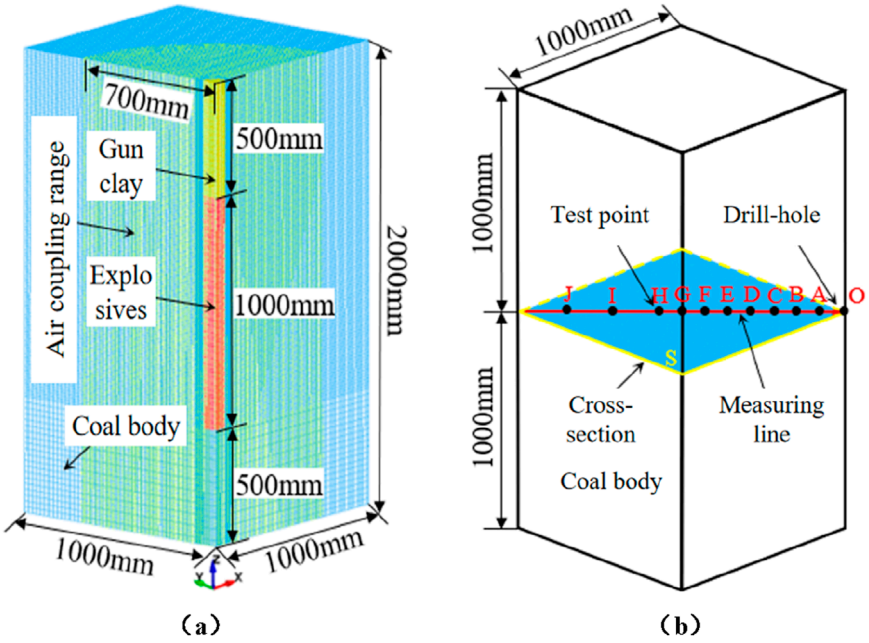

FIGURE 8
Construction of a pre-cracking model for roof blasting. **(a)** Numerical computation model. **(b)** Measurement point layout.

elastic bearing zone shrinks to zero width, it disappears entirely, causing E_{C1} to decrease to zero. The coal pillar's plastic zones then connect, placing the pillar at the critical state of overall instability. If a critical layer suddenly fractures, the released energy propagates to the coal pillar as stress waves, causing a sudden and significant reduction in bearing capacity. This can highly likely trigger overall instability and failure of the coal pillar. Therefore, the disappearance of the coal pillar's elastic bearing zone ($E_{C2} = 0$) can be regarded as the critical condition for impact-induced instability in roadways.

Based on this quantitative criterion, the following sections will delineate impact-prone zones and establish a targeted "regional-local" source-specific monitoring and prevention system to achieve dynamic risk level control.

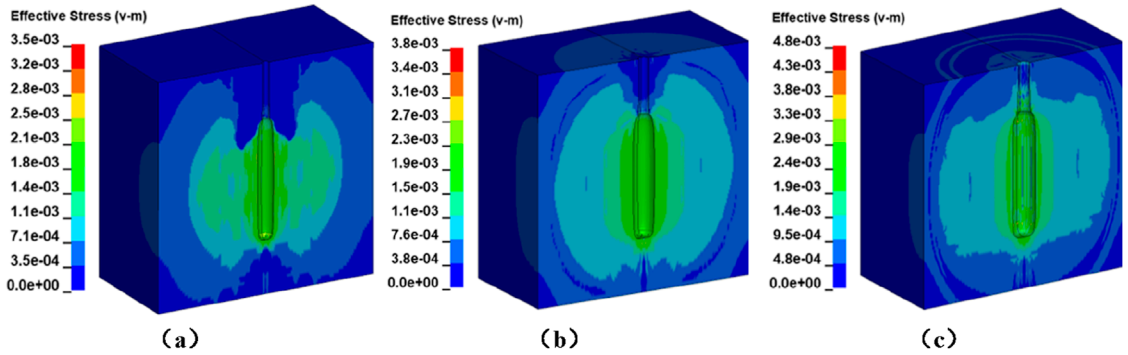

FIGURE 9
Effective stress of different charge diameter models. **(a)** Φ65 mm. **(b)** Φ75 mm. **(c)** Φ95 mm.

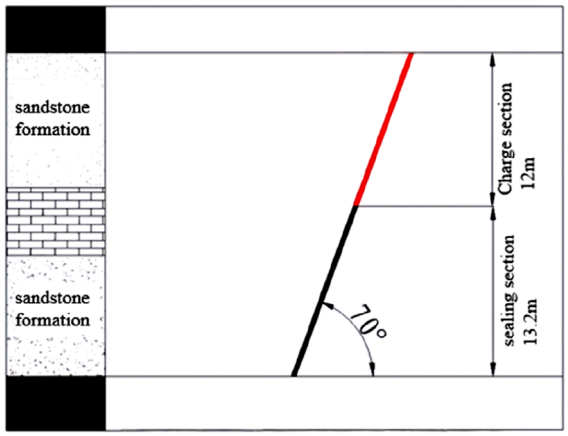

FIGURE 10
Layout of roof pre blasting.

3.4 Division of rock burst hazard areas

Combined with the rock burst initiation theory and the evaluation results of the rock burst hazard level of the 41,109 working face, it was found that although the mining working face had weak rock burst hazard, the risk of rock burst in the working face was increased due to factors such as mining disturbance, geological structure, and coal seam occurrence characteristics. Moreover, the superposition of "dynamic and static loads" was the main inducing factor. The rock burst hazard areas of the 41,109 working face were drawn through comprehensive analysis, as shown in Figure 3.

It could be seen from Figure 2 that the 41,109 working face was generally at a weak rock burst hazard during mining, but due to the influence of structural factors and mining technology, local areas (faults and structures) were at a medium rock burst hazard. To ensure safe mining, it was suggested to strengthen monitoring work in medium rock burst hazard areas, formulate special rock burst prevention measures in advance, actively take pressure relief measures, strengthen support, and do a good job in rock burst prevention.

4 Rock burst separate source monitoring scheme during working face mining

4.1 Rock burst separate source monitoring and early warning system

According to the relevant conditions of rock burst monitoring in Dafosi Coal Mine, a rock burst monitoring system combining dynamic and static load monitoring (You, 2017) had been formed. The microseismic monitoring system could conduct real-time monitoring on the concentrated dynamic load sources causing rock burst in the entire working face area. The ground sound monitoring system could conduct real-time monitoring on the concentrated dynamic load sources causing rock burst in local areas such as mining working faces.

The surrounding rock stress monitoring could conduct real-time monitoring on the concentrated static load sources causing rock burst in local areas. Therefore, for the rock burst prevention and control work during the mining period of the 41,109 working face in Dafosi Coal Mine, it was divided from three angles: load source type, monitoring range, and monitoring method. A separate source monitoring and early warning system for rock burst with "regional monitoring combined with local monitoring" was established for static and dynamic load sources (Figure 4).

4.2 Rock burst hazard monitoring scheme

4.2.1 Surrounding rock dynamic load monitoring

The ARAMIS M/E microseismic monitoring system could be used to monitor the energy release from hard roof fracture. Microseism was used to monitor the high-frequency sound waves emitted by underground roof fracture or rock stratum vibration. Real-time feedback of monitoring data was used to monitor and warn rock burst hazards. To meet the needs of microseismic monitoring, the geophones and probes of the microseismic system were arranged in a rhombus pattern and adjusted in a timely manner as the working face advanced. One microseismic geophone and one microseismic probe were arranged in the transport roadway

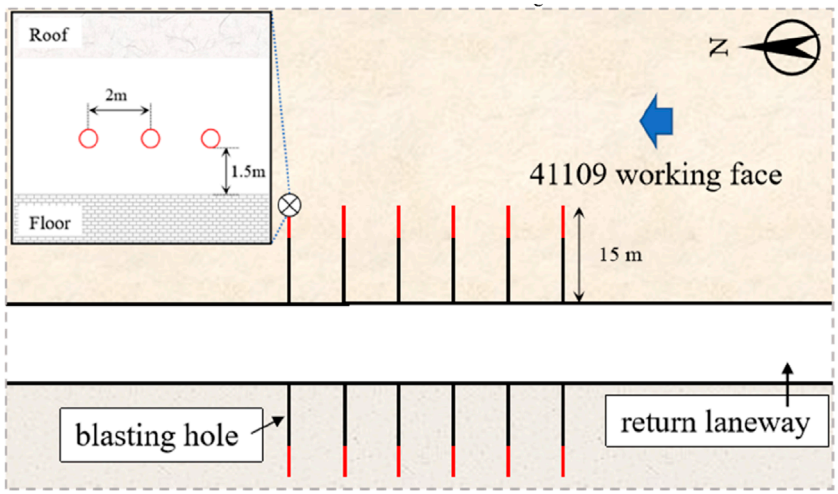

FIGURE 11
Layout of large diameter pressure relief drilling holes for the upper part.

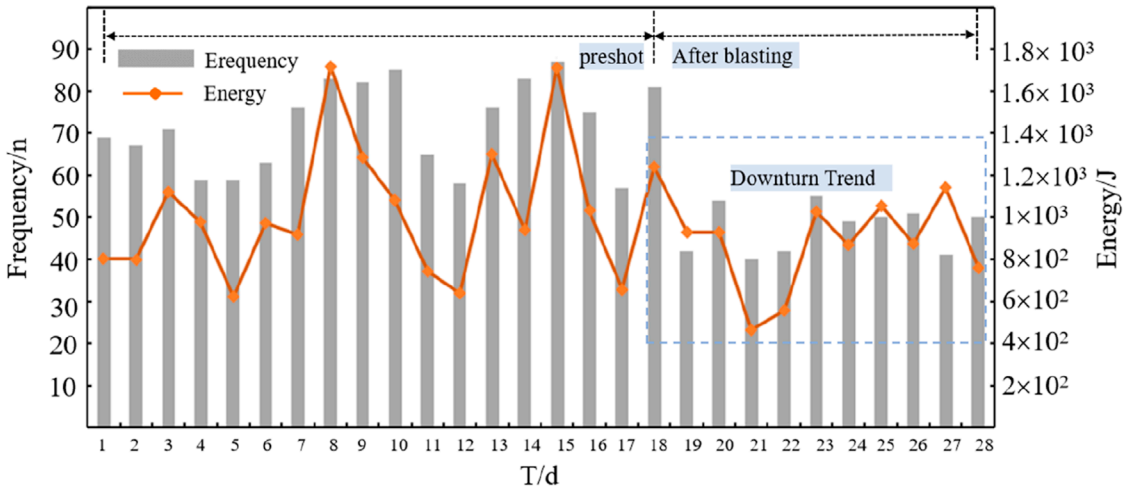

FIGURE 12
Energy frequency characteristics of microseismic events before and after roof pre blasting.

and return airway of the 41,109 working face respectively, and the geophones and probes were arranged in a rhombus pattern as far as possible (Figure 5). The distance between probes was 200–500 m, and the distance between geophones was 800–1000 m.

Since the ground sound monitoring system is sensitive to the acoustic signals of high-frequency rock fracture, it can continuously monitor the development of microcracks in rock strata and is highly sensitive to disaster occurrence, so it is widely used in mine disaster monitoring. The layout of the ground sound monitoring system for the 41,109 working face is shown in Figure 6, which can monitor the stability of the surrounding rock of the working face in real time. To maximize the monitoring advantages of ground sound, two ground sound monitoring probes were arranged in each mining roadway (Figure 6). When the working face advanced to a position 30 m near the probe, the probe was moved forward by 160 m. This cyclic movement of the sensor improved the monitoring accuracy and precision.

4.2.2 Surrounding rock static load monitoring

The KJ649 stress monitoring system was used to monitor the local static load during the mining of the working face. During the mining of the working face, the layout range of monitoring points was no less than 300 m in front of the working face, which was arranged in the two roadways of the working face. The distance between monitoring groups was no more than 30 m, and two borehole stress gauges were arranged in each group (Figure 7). The depths of the boreholes were 9 m and 14 m respectively, and the distance within the group was 1.5 m, which was used to monitor the variation of mining-induced stress during the mining process of the working face.

5 Design of rock burst separate source prevention and control scheme for working face

5.1 Determination of roof pre-splitting blasting parameters

To determine suitable roof pre-splitting blasting parameters, LS-DYNA explicit dynamic analysis software was employed to analyze the blasting effects on the roof. Due to the presence of numerous primary joints and fractures in the roof, its mechanical properties are complex. The HJC (Holmquist-Johnson-Cook) damage constitutive model was selected, which is suitable for studying the failure process and fragmentation mechanism of rock materials under dynamic loading. The explosive material was modeled using LS-DYNA's built-in∗MAT_HIGH_EXPLOSIVE_BURN high-performance explosive material model, employing the JWL equation of state to describe the relationship between volume and pressure of the explosive products during detonation. The constructed roof blasting model is illustrated in Figure 8.

To ensure the accuracy of the blasting simulation results, the following assumptions are made for the established numerical model: ① The coal body is assumed to be isotropic, meaning its physical and mechanical properties are homogeneous and continuous; ② The self-weight of the coal body is neglected; ③ The permeation of blast gases within the coal mass during detonation is disregarded; ④ No heat exchange occurs within the blast products; ⑤ Partial surfaces in the numerical model are defined as non-reflective boundary conditions, simulating an infinitely large underground coal mass within a finite computational domain.

The borehole diameter for underground blasting operations depends on the mining drill rig. The ZDY-1000G hydraulic mining drill rig is powerful, easy to operate, highly modular, and easily transportable. It offers borehole diameters of Φ65 mm, Φ75 mm, and Φ95 mm, with a spindle tilt angle ranging from −90° to 30°. This rig has been extensively utilized in drilling operations at the Dafosi Coal Mine. Considering the duration of the entire model blasting process and to facilitate observation of stress and damage evolution patterns throughout the explosion-induced fracturing weakening process, the termination calculation time is set to 3,000 μs. To ensure precise and stable computation, the time step is set to 20 μs. The entire modeling process adopted the cm-g-us unit system. Coupled charging (where explosives tightly contact the borehole) was employed, with simultaneous detonation of the entire charge. This approach achieved excellent coal fragmentation and reduced large block rates.

Single-hole blasting models with charge diameters of Φ65 mm, Φ75 mm, and Φ95 mm were sequentially established and submitted to the LS-DYNA Solver for successive calculations. To more clearly observe shock wave propagation at different time points, the upper half of the quarter model was removed from the plane perpendicular to the blast hole at Z = 1,000 using the Blank function in the LS-PREPOST menu, enabling observation of shock wave evolution over time. Figure 9 shows the pressure evolution of shock waves after blasting for models with different charge diameters.

As shown in Figure 9, the shock wave generated by the explosive detonation propagates outward from the center of the borehole while also extending along the borehole toward the hole mouth. The shock wave exhibits varying states at different time points, with an overall trend of outward expansion along the borehole. As propagation distance increases, its peak pressure gradually diminishes. As the diameter of the explosive charge increases, the radii of the fragmentation zone and fracture zone within the blasted coal body also expand. Analyzing the fissure zone radius: as charge diameter increases, the Φ65 mm borehole exhibits a fissure zone of 29 cm. For Φ75 mm to Φ95 mm boreholes, the fissure zone also shows an increasing trend, though at a slower rate. The fissure zone radius for the Φ95 mm charge diameter model is only 3 cm larger than that of the Φ75 mm borehole. Although the Φ95 mm borehole exhibits the largest fracture zone, it is not the most economical option. Considering both effectiveness and cost, it is recommended to select the Φ75 mm charge diameter for field application.

5.2 Roof pre-blasting pressure relief scheme

According to the coal seam occurrence environment and the situation of adjacent working faces, it was known that the sudden release of elastic potential energy accumulated in the roof strata during the mining process increased the stress concentration degree of the surrounding rock and increased the number of unstable factors. To weaken the dynamic load effect of the hard roof, pre-blasting was adopted to reduce the release intensity of the roof elastic energy. The specific implementation measures are shown in Figure 10.

The parameters of roof pre-blasting were as follows: a single row of blasting holes was arranged on the coal pillar side of the return air gateway of the working face, with a hole depth of 25.2 m, a vertical height of 23 m, a hole spacing of 8 m, a deviation of 14° towards the coal pillar side along the roadway strike direction, and an azimuth angle of 194°. The blasting hole diameter was 75 mm, the elevation angle was 70°, the charging length was 12 m, the hole sealing length was 13.2 m, the charge per hole was 36 kg, and yellow mud was used for hole sealing. The roof blasting pre-splitting construction area was 350 m, with a total of 44 boreholes arranged.

5.3 Large-diameter drilling weakening scheme

The surrounding rock pressure relief scheme during mining: when the working face was mined into the weak rock burst hazard area, large-diameter drilling was used for weakening to reduce the elastic energy storage capacity of the coal mass. The specific layout parameters are shown in Figure 11. The depth of the constructed borehole was 15 m, the hole inclination angle was 0°–3°, the borehole diameter was 153 mm, the borehole spacing was 2 m, and the borehole height was 1.5 m above the ground. Boreholes were arranged on both sides of the roadway at the same time, and the stagger distance of the boreholes on both sides was 1.5 m. If the pressure relief effect and efficiency were not ideal, the pressure relief parameters of the sidewall should be optimized according to the actual situation on site. To improve the pressure relief efficiency, the pressure relief boreholes were no less than 300 m ahead of the working face.

5.4 Evaluation of pressure relief effect

To test the effectiveness of the pressure relief scheme for the 41,109 working face, microseismic monitoring equipment was used to analyze the microseismic data before and after blasting. The energy and frequency characteristics of microseismic events within 1 month were plotted as shown in Figure 12.

It could be seen from Figure 12 that before roof blasting pressure relief, the energy and frequency of microseismic events were generally high. The maximum energy released by a single microseismic event was 1.7×10^3 J, and the maximum frequency was 87 times. The energy of a single microseismic event was between 0.6×10^3 J and 1.2×10^3 J. It could be seen that microseismic events were relatively frequent and accumulated a large amount of energy, increasing the degree of danger. After blasting pressure relief, the energy-frequency of microseismic events monitored on the roof decreased sharply. The energy of microseismic events was reduced by 54%, indicating that the advanced pre-blasting of the roof alleviated the energy accumulation effect and could greatly weaken the degree of roof energy accumulation. To sum up, it could be indicated that the application of advanced roof pre-blasting to control rock burst in the 41,109 working face had obvious effects and could be popularized and applied.

6 Conclusion

1. The comprehensive index method was employed to assess the rock burst hazard level of the 41,109 working face. The rock burst hazard index was determined to be 0.429 (indicating a low hazard level), consistent with the working face's rock burst susceptibility classification.
2. Considering the influence of structural factors and mining techniques, the 41,109 working face was divided into rockburst hazard zones. Based on the theory of dynamic and static load superposition, a multi-source monitoring and early warning system for rockburst hazards was established for the hazard zones, employing a "regional monitoring + local monitoring" approach.
3. Based on the energy release characteristics of dynamic-static load superposition, a source-specific prevention plan for rockburst control in the working face was designed. Pressure regulation in hazardous zones was achieved through roof deep-hole pre-blast and large-diameter drilling. This reduced microseismic energy from roof fractures by 54% compared to pre-treatment levels, effectively controlling rockburst risks and ensuring safe, efficient coal extraction in the working face.

Data availability statement

The original contributions presented in the study are included in the article/supplementary material, further inquiries can be directed to the corresponding author.

Author contributions

YY: Writing – original draft. WG: Methodology, Writing – review and editing. JF: Formal Analysis, Writing – review and editing. SZ: Writing – review and editing. BZ: Writing – review and editing.

Funding

The author(s) declare that financial support was received for the research and/or publication of this article. This study was financially supported by the Postdoctoral Fund Project of China Coal Energy Research Institute (ZMYXM∗BH-24-01). Research and Development of Surrounding Rock Control Technology and Materials for Soft Rock Roadways under the Action of Deep High Stress and High Mineralization Water (20241CY001). This project belongs to the key scientific research project of middling coal. Since the postdoctoral research fund can only meet part of the page fees, this fund is added to pay for the remaining page fees. The authors of the paper, YY, WG, BZ, are all members of the research team of this project.

Conflict of interest

Authors YY, WG, and BZ were employed by China Coal Energy Research Institute Co., Ltd.

Author JF was employed by China Railway 17th Bureau Group Second Engineering Co., Ltd.

The remaining author declares that the research was conducted in the absence of any commercial or financial relationships that could be construed as a potential conflict of interest.

Generative AI statement

The author(s) declare that no Generative AI was used in the creation of this manuscript.

Any alternative text (alt text) provided alongside figures in this article has been generated by Frontiers with the support of artificial intelligence and reasonable efforts have been made to ensure accuracy, including review by the authors wherever possible. If you identify any issues, please contact us.

Publisher's note

References

Cao, Z., Zhang, S., and Yi, X. (2025). Disaster-causing mechanism of spalling rock burst based on folding catastrophe model in coal mine. *Rock Mech. Rock Eng.*, 1–14. doi:10.1007/s00603-025-04497-6

Dai, L., Feng, D., Pan, Y., Wang, A., Ma, Y., Xiao, Y., et al. (2025). Quantitative principles of dynamic interaction between rock support and surrounding rock in rockburst roadways. *Int. J. Min. Sci. Technol.* 35 (1), 41–55. doi:10.1016/j.ijmst.2024.12.009

Feng, C., Yanbi, Y., and Lai, X. (2019). Physical similar material simulation experiment study on rock burst induced by key stratum fracture based on microseismic monitoring. *Chin. J. Rock Mech. Eng.* 38 (04), 803–814. doi:10.13722/j.cnki.jrme.2018.1423

He, S., Song, D., He, X., Chen, J., Ren, T., Li, Z., et al. (2020). Coupled mechanism of compression and prying-induced rock burst in steeply inclined coal seams and principles for its prevention. *Tunn. Undergr. Space Technol.* 98, 103327–22. doi:10.1016/j.tust.2020.103327

Huicong, X., Lai, X., Shan, P., Yang, Y., Zhang, S., Yan, B., et al. (2022). Energy dissimilation characteristics and shock mechanism of coal-rock mass induced in steeply-inclined mining: comparison based on physical simulation and numerical calculation. *Acta Geotech.* 18, 843–864. doi:10.1007/s11440-022-01617-2

Kong, L., Shang, J., Ranjith, P. G., Li, B. Q., Song, Y., Cai, W., et al. (2024). Grain-based DEM modelling of mechanical and coupled hydro-mechanical behaviour of crystalline rocks. *Eng. Geol.* 339, 107649. doi:10.1016/j.enggeo.2024.107649

Lai, X., Zhang, S., Cao, J., Sun, Y., and Xin, F. (2025). Difference of "whole-process and stages" response law of energy evolution regulated by high energy storage rock modification. *Geohazard Mech.* 3, 99–108. doi:10.1016/j.ghm.2025.06.001

Linming, D., Jiang, H., and Cao, A. (2015). Superposition principle of dynamic and static loads in coal mine rock burst and its prevention. *J. China Coal Soc.* 40 (07), 1469–1476. doi:10.13225/j.cnki.jccs.2014.1815

Linming, D., Jiang, H., and Cao, A. (2017). Stress field-vibration wave field monitoring and early warning technology for dynamic and static loads of coal mine rock burst. *Chin. J. Rock Mech. Eng.* 36 (04), 803–811. doi:10.13722/j.cnki.jrme.2016.0756

Linming, D., Kunyo, Z., and Song, S. (2021). Research on mechanism, monitoring, early warning and prevention technology of coal mine rock burst. *J. Eng. Geol.* 29 (04), 917–932. doi:10.13544/j.cnki.jeg.2021-0337

Liu, J., Yang, W., and Jiang, F. (2017). Mechanism and field experiment of preventing rock burst by cracking first and then injecting. *Chin. J. Rock Mech. Eng.* 36 (12), 3040–3049. doi:10.13722/j.cnki.jrme.2017.0206

Lu, Z., Ju, W., and Wang, H. (2019). Experimental study on anisotropic characteristics of impact tendency and failure mode of hard coal. *Chin. J. Rock Mech. Eng.* 38 (4), 757–768. doi:10.13722/j.cnki.jrme.2018.1424

Ming, C. (2024). Rockburst risk control and mitigation in deep mining. *Deep Resour. Eng.* 2 (1), 100019. doi:10.1016/j.deepre.2024.100019

Pan, J., Meihua, F., and Lu, Z. (2021). Research and application of comprehensive monitoring and early warning platform for coal mine rock burst. *Coal Sci. Technol.* 49 (6), 32–41. doi:10.13199/j.cnki.cst.2021.06.004

Pan, J., Yongxue, X., and Wang, S. (2024). Technical difficulties and emerging development directions of deep rock burst prevention in China. *J. China Coal Soc.* 49 (3), 1291–1302. doi:10.13225/j.cnki.jccs.2023.1480

Pengxiang, L. I., Wang, Z., Chen, B., Peng, J., Zhang, B., Zhao, J., et al. (2024). Rockburst hazard assessment and prevention and control strategies in the Ruihai gold mine. *Front. Earth Sci.* 11, 1348366. doi:10.3389/feart.2023.1348366

Qi, Q., Yizhe, L., and Shankun, Z. (2019). Seventy years of rock burst development in coal mines in China: establishment and consideration of theory and technology system. *Coal Sci. Technol.* 47 (9), 1–40. doi:10.13199/j.cnki.cst.2019.09.001

Qiu, J., Rui, H., Wang, H., Wang, F., and Zhou, C. (2025). Rate-dependent tensile behaviors of jointed rock masses considering geological conditions using a combined BPM-DFN model: strength, fragmentation and failure modes. *Soil Dyn. Earthq. Eng.* 195, 109393. doi:10.1016/j.soildyn.2025.109393

Tan, Y., Zhang, X., and Xiao, Z. (2024). Main control factors of rock burst and its disaster evolution mechanism. *J. China Coal Soc.* 49 (1), 367–379. doi:10.13225/j.cnki.jccs.2023.0829

Wang, H., Jiang, Y., and Daixin, D. (2017). Study on the causes of rock burst under complex geological conditions in Yima coalfield. *Chin. J. Rock Mech. Eng.* 36 (Suppl. 2), 4085–4092. doi:10.13722/j.cnki.jrme.2017.0463

Xie, H., Zhou, H., and Xue, D. (2012). Research and consideration on deep coal mining and ultimate mining depth. *J. China Coal Soc.* 37 (4), 535–542. doi:10.13225/j.cnki.jccs.2012.04.011

Xie, H., Gao, F., Ju, Y., Ge, S., Wang, G., Zhang, R., et al. (2017). Theoretical and technical conception of fluidized mining of deep underground coal resources. *J. China Coal Soc.* 42 (03), 547–556. doi:10.13225/j.cnki.jccs.2017.0299

Yang, Y., Qinqwei, L., Cheng, G., Song, Y., and Wang, M. (2024). Research on prevention and control technology of classified rockburst in TBM construction of deeply buried tunnels. *Sci. Rep.* 14 (1), 333. doi:10.1038/s41598-024-51228-y

Yongxue, X., Hang, L., and Xiangzhi, W. (2011). Study on comprehensive evaluation technology of rock burst hazard based on microseismic and ground sound monitoring. *J. China Coal Soc.* 36 (S2), 358–364. doi:10.13225/j.cnki.jccs.2011.s2.031

You, X. (2017). Impact failure of roadway surrounding rock under superposition disturbance of dynamic and static loads. *Metal. Mine* 46 (06), 56–60.

Yuan, L. (2020). Research progress on risk identification and monitoring early warning technology of typical dynamic disasters in coal mines. *J. China Coal Soc.* 45 (05), 1557–1566. doi:10.13225/j.cnki.jccs.dy20.0272

Zhang, Q., Weiguo, L., Yuan, L., Zheng, T., Liang, Z., and Wang, X. (2024a). A review of tunnel rockburst prediction methods based on static and dynamic indicators. *Nat. Hazards* 120 (12), 10465–10512. doi:10.1007/s11069-024-06657-3

Zhang, Q., Huo, J., Yuan, L., Li, Y., Yang, F., and Wang, X. (2024b). A review of rockburst prevention and control methods in tunnels: graded and classified prevention and control. *Bull. Eng. Geol. Environ.* 83 (3), 83. doi:10.1007/s10064-024-03570-8

Zhang, L., Ning, Z., Miao, S., Feng, Z., Sun, J., Cai, M., et al. (2025). Experimental and numerical investigations on the mixed-mode fracture of granite under offset three-point bending loads. *Rock Mech. Rock Eng.* doi:10.1007/s00603-025-04871-4

Zhang, S., Lai, X., Cao, J., Xu, H., Zhang, Y., Yan, B., et al. (2026). Theoretical analyses of surrounding rock stress of a non-circular tunnel considering the horizontal inclination of initial principal stress field. *Tunn. Undergr. Space Technol.* 167, 106994. doi:10.1016/j.tust.2025.106994

Zhang, L., Wang, M., and Bin, Z. (2025a). Damage mechanism of coal samples under the coupling effect of sulfate erosion and wet-dry cycles: experiments, constitutive models, and numerical simulations. *Phys. Fluids*. doi:10.1063/5.0281708

Zhang, S., Sun, Y., and Cao, J. (2025b). Research and optimization on the strength recovery mechanism of post peak fragmentation grouting reinforcement in mining rock mass. *Front. Mater.* 12. doi:10.3389/fmats.2025.1612050

Zhou, C., Yichao, R., Qiu, J., Wang, Z., Zhou, T., Long, X., et al. (2025). The role of fracture in dynamic tensile responses of fractured rock mass: insight from a particle-based model. *Int. J. Coal Sci. and Technol.* 12, 39. doi:10.1007/s40789-025-00777-2